Journal of Statistical Physics, Vol. 61, Nos. 5/6, 1990

Moments of the Percus–Yevick Hard-Sphere Correlation Function

N. E. Berger[1] **and V. Twersky**[1]

Received April 9, 1990; final July 20, 1990

A simple recursive relation is derived for the moments M_n, $n = 1, 2,...,$ of the Percus–Yevick correlation function $h(r)$ for identical hard spheres. The M_n are rational functions of the volume fraction w occupied by the spheres; the first ten are given explicitly, and a single-term asymptotic form is obtained to suffice for the rest. Applications of the $M_n(w)$ include testing different approximations for h by numerical integration of $h(r)\, r^n$. We compare exact moments with shell approximations $M_n[h^s]$ corresponding to integration from $r = 0$ to $s + 1$ for $s = 3$–8, and with hybrid approximations $M_n[h^s + h^a]$ which supplement the shell approximations with integrals of an asymptotic tail from $s + 1$ to ∞. For a given s, the hybrid approximation is better for w increasing than the shell approximation, and $M_n[h^3 + h^a]$ is even better than $M_n[h^8]$.

KEY WORDS: Percus–Yevick correlation function; moments; shell expansions; asymptotic forms; residue series; hybrid approximations.

1. INTRODUCTION

The solution of the Percus–Yevick (PY) equation(1) for the radial distribution function $g(r)$ of a classical fluid of identical hard spheres was obtained by Wertheim(2) and by Thiele(3) in terms of the Laplace transform $\mathscr{L}\{rg(r)\} = G(t)$. Here r is the distance from the center of one sphere divided by the sphere diameter d, so that $g(r) = 0$ for $r < 1$, and $g(r) = g(w; r)$ depends on only one parameter: the volume fraction occupied by the spheres, $w = \rho\pi d^3/6$, with ρ the number density. Piecewise analytic expressions for $g(r)$ at given r in the shells $s < r < s + 1$ for $s = 1, 2,...,$ can be obtained(2) by expanding the inverse transform $\mathscr{L}^{-1}\{G(t)\}$ in a geometrical progression and summing the residues of the

[1] Mathematics Department, University of Illinois, Chicago, Illinois 60680.

0022-4715/90/1200-1187$06.00/0

terms (g_m) from $m=1$ to s. The exact results in the range $0 \leqslant r < s+1$ will be indicated by g^s.

Wertheim gave the closed from for g_1, and analogs through g_5 and tabulated values are available[4–6] for $r \leqslant 6$. Such shell expansions have relatively broad applicability, but we found them unsuitable except for small w for numerical investigations of integral equations[7] for multiple scattering by correlated random distributions of spherical resonators. We extended the shell development to g_8, considered the residue series for the complete[2] $\mathscr{L}^{-1}\{G\}$ (which exhibits a Gibbs-like effect near $r=1$, but whose leading term g^a for moderately large r approximates g^s), as well as a hybrid approximation (g^b) based on g^s for $r \leqslant s+1$ and g^a for $r > s+1$. Although these extensions suffice for larger w than g^5, the most stable computational routines we developed for even moderately large w were based on the moments M_n of the total correlation function $h = g-1$. The present paper deals primarily with the moments and their applications to test shell (h^s) and hybrid (h^b) forms of h by numerical integration.

The moments

$$M_n = \int_0^\infty dr\, h(w; r)\, r^n = M_n(w), \qquad h = g-1 \tag{1}$$

are simple rational functions of w. The first three are available in the literature,[4,8,9] and we may reconstruct these and obtain additional moments by symbolic computer differentiation of $\mathscr{L}\{rh(r)\} = H(t)$. However, it is much more convenient to work with a recursive relation for the M_n based on Baxter's equation[10] for the PY h.

Section 2 provides a form of $H(t)$ suitable for symbolic differentiation, and then derives the recursive relation for the M_n. The first ten moments $M_n(w)$ are displayed in Fig. 1 and listed in the Appendix. Section 3 derives an asymptotic series $M_n \sim \sum_\nu M_n^\nu$ for large n based on the residues at the roots $t_\nu(w)$ of the denominator[2] of $H(t)$. Figure 2 graphs the first five roots, and Table I provides numerical values for the dominant root $t_1(w)$ (and for basic magnitude U_1 and phase u_1 functions); a one-term approximation M_n^1 suffices for $n > 6$ and $w > 0.01$. Section 4 considers shell expansions $g^s = h^s + 1$ and compares exact $M_n(w)$ with shell approximations $M_n[h^s]$ based on numerical integration of $h^s r^n$ from $r=0$ to $s+1$ for $s = 3$–8. Figure 3 displays $g(w; r)$ to $r=9$ and $w=0.6$, and Fig. 4 compares $M_2[h^s]$ and $M_6[h^s]$ with the exact moments. Section 5 considers the convergent residue for $h(r) = \sum_\nu h^{(\nu)}$. Figure 5 compares exact shall results with residue sequences for $w=0.2$ and 0.6 to show the Gibbs-like effect near the discontinuity at $r=1$. Figure 6 shows that the leading residue term $h^{(1)} = h^a$ (which follows directly from Table I) suffices for $r > 5$ even for $w = 0.6$.

Figure 4 also shows that the hybrid $M_6[h^s + h^a] = M_6[h^s] + \int_{s+1}^{\infty} dr\, h^a r^6$ approximation is much better than the shell approximation for a given s, and that $M_6[h^3 + h^a]$ is even better than $M_6[h^8]$; the hybrid curves for M_2 included in Fig. 4 practically overlay the exact results.

2. MOMENTS OF THE CORRELATION FUNCTION

The exact leading terms of h for small w equal[11]

$$\begin{aligned} h &= -1, & 0 \leqslant r < 1 \\ h &= w(8 - 6r + r^3/2) + \mathcal{O}(w^2), & 1 \leqslant r < 2 \end{aligned} \tag{2}$$

which also follow from the PY equation.[1] Substituting in (1), we obtain

$$M_n = -\frac{1}{n+1} + w\,\frac{2^{n+5}3 - (5n^2 + 39n + 82)}{2(n+1)(n+2)(n+4)} + \mathcal{O}(w^2) \tag{3}$$

The exact w^2 contribution to h is also known[12] in terms of elementary functions, and the PY approximation can be identified directly by comparison of forms in refs. 12 and 1. Although such expansions of h suffice for small w, (3) indicates that corresponding expansions of M_n are restricted to smaller w as n increases. In the following we consider closed forms of $M_n(w)$ for the PY h without restrictions on w or n.

The generating function of the moments is $\mathscr{L}\{rh(r)\} = H(t)$:

$$\begin{aligned} H(t) &= \int_0^{\infty} dr\, rh(r)\, e^{tr} = \sum_{n=0}^{\infty} \frac{(-t)^n}{n!} \int_0^{\infty} dr\, h(r)\, r^{n+1} \\ &= \sum_{n=1}^{\infty} \frac{(-t)^{n-1}}{(n-1)!} M_n \end{aligned} \tag{4}$$

$$M_n = (-1)^{n-1} \lim_{t \to 0} \frac{d^{n-1}}{dt^{n-1}} H(t) \tag{5}$$

From Wertheim,[2] we write $\mathscr{L}\{rg\} = G$ in the form

$$G(t) = tL(t)/D(t), \qquad D(t) = 12wL(t) + S(t)\, e^t, \tag{6}$$

where

$$S(t) = (1-w)^2 t^3 + 6w(1-w)\, t^2 + 18w^2 t - 12w(1-w)$$

$$L(t) = (1 + w/2)t + 1 + 2w$$

Thus

$$H(t) = G(t) - t^{-2} = tL(t)/D(t) - t^{-2} \tag{7}$$

and (5) may be performed by machine[13] operations on the equivalent form

$$H(t) = \frac{L(t)[E_2(t) - 12wE_5(t)] - (1 + w/2)^2}{[1 + 12wtE_4(t)]\, L(t) - t(1 + 2w)(1 + w/2)} \tag{8}$$

where

$$E_n(t) = t^{-n}\left[e^{-t} - \sum_{\nu=0}^{n-1} (-t)^\nu/\nu!\right]$$

The Fourier transform representation of the structure factor

$$\begin{aligned} F(K) &= 1 + (6w/\pi) \int d\mathbf{r}\; h(r) \exp(i\mathbf{K}\cdot\mathbf{r}) \\ &= 1 + (24w/K) \int_0^\infty dr\; rh(r) \sin(Kr) \end{aligned} \tag{9}$$

generates the even moments

$$F(K) = 1 + 24w \sum_{n=1}^{\infty} \frac{(-K^2)^{n-1}}{(2n-1)!} M_{2n} = 1 + 24wM_2 - 24w \frac{K^2 M_4}{3!} + \cdots \tag{10}$$

Since $F(K) = F(w; K)$ must vanish for the unrealizable bound $w = 1$ (corresponding to zero fluctuation scattering for a uniform medium), we require $M_2(1) = -1/24$ and $M_{2n}(1) = 0$ for $n \geqslant 2$. The PY F is also known in closed form[14]; in particular,

$$F(w; 0) = \frac{(1-w)^4}{(1+2w)^2} = 1 + 24wM_2(w) \tag{11}$$

vanishes at $w = 1$. Equation (11), which also follows[15] directly from the scaled particle[16] equation of state, gives $M_2(w)$ in closed form[4] by inspection. The remaining PY M_{2n} are found to have $F(w; 0)$ as a factor.

A simpler representation of the M_n follows from Baxter's equation[10]

$$rh(r) = -q'(r) + 12w \int_0^1 dt\; (r-t)\, h(|r-t|)\, q(t) \tag{12}$$

where

$$q(r)(1-w)^2 = (1+2w)(r^2 - 1) - (3w/2)(r-1)$$

with $q(r) = 0$ for $r \geqslant 1$, and $q'(r) = dq/dr$. Operating on rh with $\int_0^\infty dr\, r^{n-1}$, changing the order of r and t integrations, and using $h(|r-t|)=-1$ for $r<t$, yields

$$M_n = -\int_0^1 dr\, q'(r)\, r^{n-1} + 12w \int_0^1 dt\, q(t) \left[\frac{t^{n+1}}{n(n+1)} + \int_t^\infty dr\, r^{n-1}(r-t)\, h(r-t) \right] \tag{13}$$

Integrating over $s=r-t$ to obtain

$$\sum_{m=0}^{n-1} \binom{n-1}{m} t^m M_{n-m}$$

we define

$$-\int_0^1 dr\, q'(r)\, r^{n-1} = \frac{A}{(1-w)^2}, \qquad A_n \equiv \frac{-[2n+(n-3)w]}{2n(n+1)}$$

$$\int_0^1 dt\, q(t)\, t^m = \frac{B_m}{(1-w)^2}, \qquad B_m \equiv -\frac{-[4+2m+(m-1)w]}{2(m+1)(m+2)(m+3)} \tag{14}$$

$$C_n = A_n + 12w \frac{B_{n+1}}{n(n+1)} = \frac{(n^2+9n+26)[3w-n(2+w)]-12(2+w)^2}{2(n+1)(n+2)(n+3)(n+4)}$$

Thus (13) reduces to

$$M_n(1-w)^2 = C_n + 12w \sum_{m=0}^{n-1} \binom{n-1}{m} B_m M_{n-m} \tag{15}$$

and shifting the $m=0$ term $12wB_0M_n = -w(4-w)\,M_n$ to the left side gives

$$M_n(1+2w) = C_n + 12w \sum_{m=0}^{n-1} \binom{n-1}{m} B_m M_{n-m} \tag{16}$$

such that $M_1 = C_1/(1+2w)$, $M_2 = (C_2 + 12wB_1M_1)/(1+2w)$, etc.

It is clear from (16) and (3) that all moments have the form

$$M_n(w) = \frac{-\mu_n(w;N)}{(n+1)(1+2w)^n}, \qquad \mu_n(w;N) = 1 + \sum_1^N a_\nu(-w)^\nu \tag{17}$$

where the polynomial μ_n of order N is given by

$$\mu_n = c_n - \sum_1^{n-1} \binom{n-1}{m} \frac{n+1}{n+1-m} b_m \mu_{n-m} \tag{18}$$

with $c_n = -(n+1)\,C_n(1+2w)^{n-1}$, and $b_n = -12wB_n(1+2w)^{n-1}$. All c_n, and b_n except b_1 (which is proportional to w), are of order $n+1$ in w; the order of μ_n (in general that of $b_2\mu_{n-2}$) is $N=(3n+1)/2$ for n odd, and $N=3n/2$ for n even.

The Appendix lists the first ten moments (generated by machine[13]), and Fig. 1 provides a three-dimensional display to delineate trends. For $0<w<1$, the number of extrema (and zeros) is given by $N-n-2>0$, so that successive pairs from M_5, M_6, to M_{19}, M_{20} start with one extremum and end with eight extrema, etc.

3. ASYMPTOTIC FORM OF M_n

Since the recursive relation for M_n involves sequential determination of preceding moments, we derive an asymptotic series for large n by working with the residues at the complex roots (t_ν, t_ν^*) of $D(t)$ in (6).

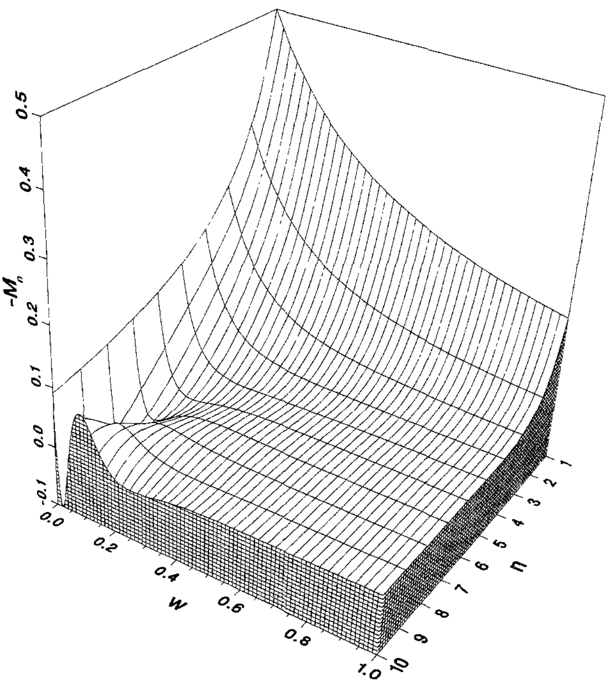

Fig. 1. Three-dimensional display to delineate trends of the first ten moments $M_n(w)$ of the hard-sphere PY h vs. volume fraction w. The values of $-M_n(0)$ are $(1+n)^{-1}$. The values of $-M_n(1)$ for $n=1, 2, 3$ are 3/20, 1/24, 3/350; the remaining even moments vanish, and the odd are small and alternate in sign.

As indicated by Wertheim,[2] $t_\nu = -\alpha_\nu + i\beta_\nu = -|\alpha_\nu| + i\,|\beta_\nu|$ such that as $w \to 1$, $\alpha = 0$, and $\beta/2 = \tan(\beta/2)$. Backtracking the branches numerically yields curves versus w in Fig. 2 that show $|t_{\nu+1}| > |t_\nu|$ for the corresponding simple poles for all w.

Thus, for large n, from

$$M_n = (-1)^n \frac{(n-1)!}{2\pi i} \oint dt\, H(t)\, t^{-n} \tag{19}$$

for a contour around 0 of radius greater than any $|t_\nu(w)|$ of interest, we obtain[17]

$$M_n \sim (-1)^n\,(n-1)!\; 2\,\mathrm{Re} \sum_\nu t_\nu^{-n+1} L_\nu / D'_\nu \equiv \sum M_n^\nu \tag{20}$$

where

$$D'_\nu = \lim_{t \to t_\nu} \frac{dD(t)}{dt} = 12wL'_\nu + (S_\nu + S'_\nu)\, e^{t_\nu}$$

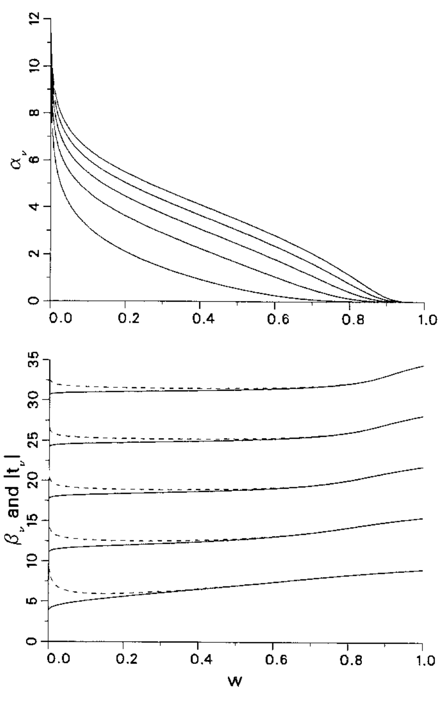

Fig. 2. First five roots $t_\nu = -\alpha_\nu + i\beta_\nu$ vs. $w \geq 0.001$. Top panel shows α_ν, and bottom panel shows β_ν (solid curves) and $|t_\nu|$ (dashed curves); the lowest curves correspond to $\nu = 1$ and the highest to $\nu = 5$. The values at $w = 10^{-6}$ are: $\alpha_\nu = 17.109$, 17.396, 17.777, 18.149, 18.484; $\beta_\nu = 3.537$, 10.483, 17.218, 23.803, 30.296.

with $S_\nu = S(t_\nu)$, etc. We write

$$M_n^\nu = (-1)^n (n-1)! \, |t_\nu^{-n}| \, U_\nu \cos(u_\nu + n\tau_\nu) \tag{21}$$

with $U_\nu e^{iu_\nu} = 2t_\nu L_\nu / D'_\nu$ and $\tau_\nu = \tan^{-1}(\beta_\nu/\alpha_\nu)$. For $n > 6$, the curves of $M_n^1(w)$ and $M_n(w)$ are indistinguishable for $0.01 \leqslant w \leqslant 1$ on the scale of Fig. 1; we may use M_n^1 for $n \geqslant 10$ and $w \geqslant 10^{-3}$, and for $n \geqslant 15$ and $w \geqslant 10^{-6}$. Except for $n = 1$, we can obtain better accord for small w by

Table I. Data[a] versus w for Dominant Root $t_1 = -\alpha + i\beta = |t| \, e^{-i\tau}$ and for $2t_1 L_1/D'_1 = Ue^{iu}$

w	α	β	$\|t\|$	τ	U	u
0.0001	11.84249	3.72491	12.41449	0.30474	24253.0	−0.25294
0.0010	9.10273	3.90913	9.90661	0.40563	2001.6	−0.31918
0.0100	6.24844	4.25717	7.56085	0.59808	158.03	−0.43333
0.0200	5.35555	4.42760	6.94878	0.69083	72.747	−0.48600
0.0300	4.82227	4.55123	6.63083	0.75649	46.067	−0.52353
0.0400	4.43754	4.65285	6.42968	0.80908	33.261	−0.55417
0.0500	4.13469	4.74131	6.29092	0.85364	25.811	−0.58078
0.0600	3.88386	4.82086	6.19073	0.89263	20.968	−0.60474
0.0700	3.66906	4.89396	6.11660	0.92748	17.581	−0.62681
0.0800	3.48070	4.96214	6.06120	0.95910	15.088	−0.64747
0.0900	3.31259	5.02646	6.01985	0.98810	13.181	−0.66706
0.1000	3.16050	5.08765	5.98941	1.01493	11.678	−0.68579
0.1250	2.83234	5.23028	5.94794	1.07448	9.0321	−0.72988
0.1500	2.55722	5.36226	5.94081	1.12581	7.3201	−0.77130
0.1750	2.31893	5.48696	5.95685	1.17094	6.1290	−0.81100
0.2000	2.10781	5.60652	5.98966	1.21119	5.2573	−0.84961
0.2500	1.74428	5.83581	6.09091	1.28036	4.0770	−0.92497
0.3000	1.43679	6.05802	6.22607	1.33793	3.3263	−0.99929
0.3500	1.17010	6.27791	6.38602	1.38653	2.8173	−1.07338
0.4000	0.93590	6.49865	6.56570	1.42776	2.4586	−1.14738
0.4500	0.72980	6.72232	6.76182	1.46266	2.2010	−1.22080
0.5000	0.54986	6.95002	6.97174	1.49184	2.0159	−1.29245
0.5500	0.39577	7.18180	7.19270	1.51575	1.8852	−1.36043
0.6000	0.26817	7.41634	7.42119	1.53465	1.7967	−1.42215
0.6500	0.16787	7.65077	7.65261	1.54886	1.7403	−1.47463
0.7000	0.09470	7.88068	7.88125	1.55878	1.7062	−1.51534
0.7500	0.04656	8.10097	8.10111	1.56505	1.6848	−1.54326
0.8000	0.01898	8.30727	8.30729	1.56851	1.6673	−1.55959
0.8500	0.00585	8.49741	8.49741	1.57011	1.6479	−1.56738
0.9000	0.00111	8.67203	8.67203	1.57067	1.6247	−1.57016
0.9500	0.00007	8.83390	8.83390	1.57079	1.5987	−1.57076
1.0000	0.00000	8.98682	8.98682	1.57080	1.5720	−1.57080

[a] The values specify the moments for large n and the correlation function for large r.

retaining additional terms in v; however, since the exact $M_n(w)$ are known, we consider only M_n^1. Supressing the subscript $v=1$, we have

$$M_n \sim M_n^1 \equiv M_n^a = (-1)^n (n-1)! \, |t^{-n}| \, U \cos(u + n\tau) \tag{22}$$

Table I lists w and values for $t_1 = t = -\alpha + i\beta = |t| \, e^{-i\tau}$, and for the corresponding $U(w)$ and $u(w)$. This table is also appropriate for a following development of h.

4. SHELL EXPANSIONS OF g

As discussed by Wertheim,[2] $g(r)$ can be obtained in closed form for given r from $\mathscr{L}^{-1}\{G\}$ by expanding G of (6) in powers of S^{-1} and evaluating the residues at the roots ($t_0 = |t_0|$, t_1, $t_2 = t_1^*$) of $S(t)$. Thus, for $r \geqslant 1$,

$$g(r) = \sum_1^{\infty} g_m(r), \qquad g^s(r) = \sum_1^{s} g_m(r) \quad \text{for } r \leqslant s+1 \tag{23}$$

such that $g_m(r) = 0$ for $r < m$, and for $r \geqslant m$,

$$r g_m(r) = \frac{(-12w)^{m-1}}{(m-1)!} \sum_{l=0}^{2} \lim_{t \to t_l} \frac{d^{m-1}}{dt^{m-1}} \left\{ (t - t_l)^m \, t \left[\frac{L(t)}{S(t)} \right]^m e^{t(r-m)} \right\} \tag{24}$$

where $g_m(m) = 0$ for $m > 1$. The results may be expressed as

$$r g_m(r) = \sum_{l=0}^{2} C_l(m, 0) \, e^{t_l(r-m)} \sum_{k=1}^{m} C_l(m, k)(r-m)^{k-1} \tag{25}$$

Wertheim[2] gives forms of the coefficients for $m = 1$, and forms for $m \leqslant 5$ are given by Smith and Henderson,[4,5] who include numerical comparisons of shell integrations and M_2 for several values of w; numerical tables for $g(w; r)$ are given in ref. 6.

Corresponding forms for the C_l for $m \leqslant 8$ (obtained by machine computations[13]) are implicit in Fig. 3, which displays $g(w; r)$ to $r = 9$ and $w = 0.6$. The first minimum of g equals zero at $w \approx 0.61257 \equiv w_0$ (for $r \approx 1.3094$), and g is negative[6] and physically unrealistic at slightly larger w. [The measured[18] values of w for loose and dense random close packing of ball bearings (0.60 ± 0.02 and 0.63 ± 0.01) bracket w_0.]

The correlation function for r in one of the first s shells is given by

$$h^s(r) = -1 + g^s(r) = -1 + \sum_{m=1}^{s} g_m(r), \qquad 1 \leqslant r \leqslant s+1 \tag{26}$$

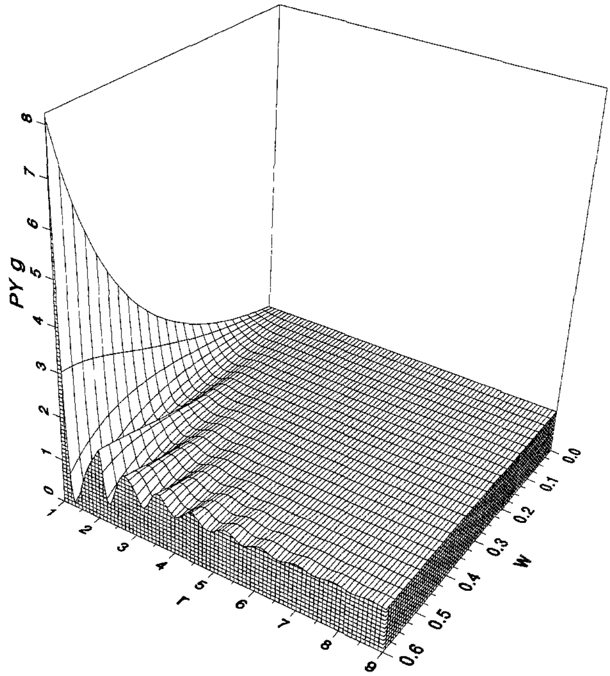

Fig. 3. Plot of PY $g(w; r)$ for $0 < w \leqslant 0.6$ and $1 \leqslant r \leqslant 9$. At $r = 1$, the curve of $g(w; 1)$ is the PY closed form $(1 + w/2)/(1 - w)^2$.

We obtain s-shell approximations for the moments by numerical integration,

$$M_n[h^s] \equiv \int_0^{s+1} dr\, h^s(r)\, r^n \tag{27}$$

and compare with the exact M_n to obtain ranges of validity $0 \leqslant w \leqslant w(s, n)$. For given n, $w(s, n)$ increases moderately with increasing s; for given s, $w(s, n)$ decreases markedly with increasing n. The essentials are indicated by the dashed curves $s = 3$–8 in Fig. 4 for $M_2[h^s]$ and $M_6[h^s]$. (The dotted curves will be discussed subsequently.)

5. RESIDUE SERIES FOR g

Wertheim[2] also considered the poles of $\mathscr{L}^{-1}\{G\}$ at the roots of $D(t)$ and indicated that the behavior of $h(r)$ for large r would be determined by

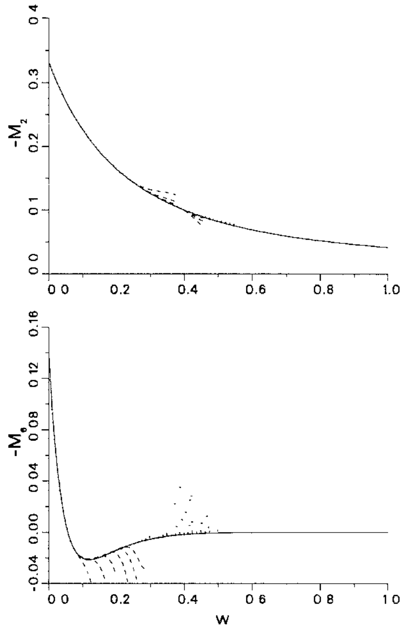

Fig. 4. The dashed curves that depart from the exact solid curves $M_2(w)$ and $M_6(w)$ at increasing values of w correspond to increasing the number of shell terms (from $s = 3$ to 8) in the approximate $M_n[h^s]$ of (27). The dotted curves that depart at larger values of w are based on the hybrid approximation $M_6[h^s + h^a]$ as in (31). The hybrid $M_6[h^3 + h^a]$ is even better than $M_6[h^8]$. The hybrid $M_2[h^s + h^a]$ curves practically overlay the exact M_2.

the pair of complex roots closest to the imaginary axis. For $r > 1$, and symbols as for (20) and (21),

$$rh(r) = 2\,\mathrm{Re} \sum_{\nu=1}^{\infty} t_\nu L_\nu e^{rt_\nu}/D'_\nu = \sum_\nu U_\nu e^{-r\alpha_\nu} \cos(r\beta_\nu + u_\nu) \equiv r \sum_\nu h^{(\nu)} \quad (28)$$

with roots $t_\nu = -\alpha_\nu + i\beta_\nu$ as in Fig. 2. This residue series is rapidly convergent except in the neighborhood of $r = 1$ (the single discontinuity of h) where successive sequences exhibit a Gibbs-like effect. For any finite number (ν') of terms, the peak of g occurs for $r > 1$; as ν' increases (a larger ν' is required for larger w), the peak approaches $r = 1$ and its magnitude overshoots the PY $g(1) = (1 + w/2)/(1 - w)^2$. Figure 5 for $w = 0.2$ and 0.6 shows the essentials for $\nu' = (1, 5, 10, 100)$; the overshoot at $r \approx 1.005$ for $\nu' = 100$ is about 9% for the smaller w and 9.4% for the larger.

For large r and $w < 1$, we need retain only the least damped exponential term

$$rh(r) \approx 2\,\mathrm{Re}(t_1 L_1 e^{rt_1}/D'_1) = Ue^{-r\alpha} \cos(\beta r + u) = rh^{(1)} \equiv rh^a(r) \quad (29)$$

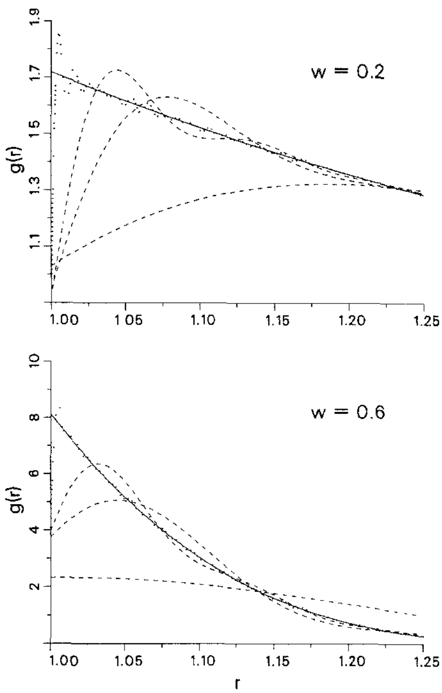

Fig. 5. Comparison of the exact $g(r)$ (solid curves) for $w=0.2$ and $w=0.6$ with v'-term residue sequence approximations (dashed or dotted curves) of (28) for $v'=(1, 5, 10, 100)$ to show the Gibbs-like effect; with increasing v', the approximations improve except for $r \approx 1$. The peak of the dotted curves ($v'=100$) at $r \approx 1.005$ overshoots the PY g values of 1.708 and 7.805 for $w=0.2$ and 0.6 by about 8.985% and 9.395%, respectively.

The subscript 1 is suppressed, and Table I applies for U, u, α, and β. As shown in Fig. 6, h^a suffices for $r>3$ at $w=0.2$, and for $r>5$ at $w=0.6$. Thus, h^a supplements the shell expansion by an asymptotic tail, and provides a hybrid approximation $h \approx h^b$ for all r. For simplicity, we use

$$\begin{aligned} h^b(r) &= h^s(r) \qquad \text{for} \quad 1 \leqslant r \leqslant s+1 \\ h^b(r) &= h^a(r) \qquad \text{for} \quad r > s+1 \end{aligned} \tag{30}$$

The corresponding hybrid approximation of the moments equals

$$M_n[h^s + h^a] = M_n[h^s] + \int_{s+1}^{\infty} dr\, h^a(r)\, r^n \tag{31}$$

where we may integrate $h^a r^n$ directly. Figure 4 compares dashed curves $M_6[h^s]$ and dotted curves $M_6[h^s + h^a]$ for $s = 3$–8 with the exact solid

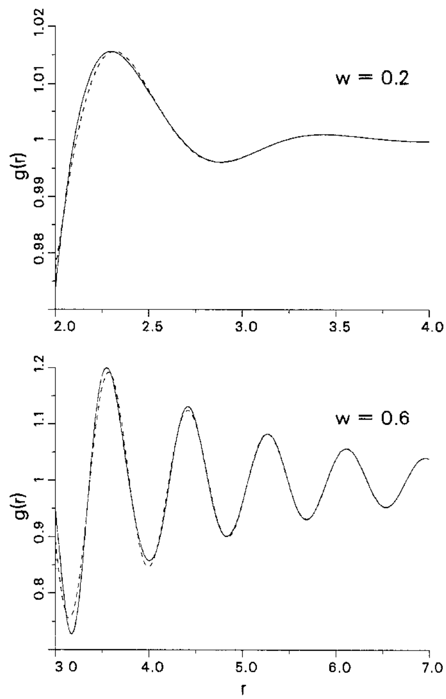

Fig. 6. Comparison of the exact g (solid curve) and leading residue term $g^{(1)} = g^a$ (dashed curve) based on (29) for $w = 0.2$ and $w = 0.6$. The one-term approximation g^a suffices at $w = 0.2$ for $r > 3$ and at $w = 0.6$ for $r > 5$.

curve M_6; for given s, the hybrid approximation holds for larger w, and $M_6[h^3 + h^a]$ is even better than $M_6[h^8]$. The hybrid dotted curves $M_2[h^s + h^a]$ in Fig. 4 practically overlay the exact solid curve M_2. The hybrid is better than the shell approximation because h^b reduces the effects of the discontinuity of h^s at $r = s + 1$; an improved version may follow from a different match-up point than $s + 1$, but this has not been investigated.

APPENDIX. MOMENTS OF THE PY TOTAL CORRELATION FUNCTION h

$$M_1 = -\frac{10 - 2w + w^2}{10 \cdot 2(1 + 2w)}$$

$$M_2 = -\frac{(4 - w)(2 + w^2)}{8 \cdot 3(1 + 2w)^2} = -\frac{8 - 2w + 4w^2 - w^3}{8 \cdot 3(1 + 2w)^2}$$

$$M_3 = -\frac{(175 - 260w + 421w^2 - 229w^3 + 62w^4 - 7w^5)}{175 \cdot 4(1+2w)^3}$$

$$M_4 = -\frac{(1-w)^4\,(16 - 11w + 4w^2)}{16 \cdot 5(1+2w)^4}$$

$$\begin{aligned} M_5 = -(&10500 - 117500w + 346930w^2 \\ &- 557372w^3 + 518840w^4 - 297700w^5 \\ &+ 101255w^6 - 17130w^7 + 756w^8)/10500 \cdot 6(1+2w)^5 \end{aligned}$$

$$M_6 = -\frac{(1-w)^4\,(20 - 386w + 627w^2 - 494w^3 + 173w^4 - 21w^5)}{20 \cdot 7(1+2w)^6}$$

$$\begin{aligned} M_7 = -(&404250 - 18203500w + 148479200w^2 \\ &- 507844540w^3 + 996929822w^4 \\ &- 1246675192w^5 + 1040639978w^6 - 582685390w^7 \\ &+ 212379965w^8 - 46596616w^9 + 5053356w^{10} \\ &- 116424w^{11})/404250 \cdot 8(1+2w)^7 \end{aligned}$$

$$\begin{aligned} M_8 = -&(1-w)^4\,(800 - 63540w + 620112w^2 \\ &- 1497976w^3 + 1841640w^4 - 1271145w^5 \\ &+ 495980w^6 - 97656w^7 + 6048w^8)/800 \cdot 9(1+2w)^8 \end{aligned}$$

$$\begin{aligned} M_9 = -(&500500 - 75540500w + 1560277375w^2 \\ &- 11161907350w^3 + 41072677500w^4 \\ &- 93389033916w^5 + 142984464462w^6 \\ &- 153929553204w^7 + 118569194898w^8 \\ &- 65226852406w^9 + 25074984188w^{10} \\ &- 6408278266w^{11} + 983239972w^{12} \\ &- 71735664w^{13} + 1009008w^{14})/500500 \cdot 10(1+2w)^9 \end{aligned}$$

$$\begin{aligned} M_{10} = -&(1-w)^4\,(2800 - 743900w + 20841976w^2 \\ &- 154963970w^3 + 456008728w^4 \\ &- 745392368w^5 + 753789316w^6 - 489600083w^7 + 201915820w^8 \\ &- 49540524w^9 + 6150144w^{10} - 232848w^{11})/2800 \cdot 11(1+2w)^{10} \end{aligned}$$

ACKNOWLEDGMENT

This work was supported in part by the Office of Naval Research.

REFERENCES

1. J. K. Percus and G. J. Yevick, Analysis of classical statistical mechanics by means of collective coordinates, *Phys. Rev.* **110**:1–13 (1958).
2. M. S. Wertheim, Exact solution of the Percus–Yevick integral equation for hard spheres, *Phys. Rev. Lett.* **10**:321–323 (1963).
3. E. Thiele, Equation of state for hard spheres, *J. Chem. Phys.* **39**:474–479 (1963).
4. W. R. Smith and D. Henderson, Analytical representation of the Percus–Yevick hard-sphere radial distribution function, *Mol. Phys.* **19**:411–415 (1970).
5. D. Henderson and W. R. Smith, Exact analytical formulas for the distribution functions of charged hard spheres in the mean spherical approximation, *J. Stat. Phys.* **19**:191–200 (1978).
6. G. J. Throop and R. J. Bearman, Numerical solution of the Percus–Yevick equation for the hard sphere potential, *J. Chem. Phys.* **42**:2408–2411 (1965); F. Mandel, R. J. Bearman, and M. Y. Bearman, Numerical solution of the Percus–Yevick equation for the Lennard-Jones (6–12) and hard sphere potentials, *J. Chem. Phys.* **52**:3315–3323 (1970).
7. V. Twersky, Coherent scalar field in pair-correlated random distributions of aligned scatterers, *J. Math. Phys.* **18**:2468–2486 (1977); *J. Acoust. Soc. Am.* **64**:1710–1719 (1978).
8. H. D. Jones, Method of finding the equation of state of liquid metals, *J. Chem. Phys.* **55**:2640–2642 (1971).
9. I. Nezbeda, Analytical solution of the Percus–Yevick equation for fluid and hard spheres, *Czech J. Phys. B* **24**:55–62 (1974).
10. R. J. Baxter, Orenstein–Zernike relation for a disordered fluid, *Aust. J. Phys.* **21**:563–569 (1968).
11. J. G. Kirkwood, Statistical mechanics of fluid mixtures, *J. Chem. Phys.* **3**:300–313 (1935).
12. B. R. A. Nijboer and L. van Hove, Radial distribution function of a gas of hard spheres and the superposition approximation, *Phys. Rev.* **85**:777–783 (1952).
13. Symbolic manipulation package **Reduce**, Version 3.2, Rand Corporation, Santa Monica, California (1985).
14. N. W. Ashcroft and J. Lekner, Structure and resistivity of liquid metals, *Phys. Rev.* **145**:83–90 (1966).
15. S. W. Hawley, T. H. Kays, and V. Twersky, Comparison of distribution functions from scattering data on different sets of spheres, *IEEE Trans. Antennas Propagation* **AP-15**:118–135 (1967).
16. H. Reiss, H. L. Frisch, and J. L. Lebowitz, Statistical mechanics of rigid spheres, *J. Chem. Phys.* **31**:369–380 (1959).
17. P. Henrici, *Applied Computational Complex Analysis*, Vol. 2 (Wiley, New York, 1977), pp. 442ff.
18. G. David Scott, Packing of spheres, *Nature* **188**:908–909 (1960).